Kinetics of Folding of Escherichia coli OmpA from Narrow to Large Pore Conformation in a Planar Bilayer †

ARTICLE *in* BIOCHEMISTRY · JUNE 2005

Impact Factor: 3.02 · DOI: 10.1021/bi047278e · Source: PubMed

2 AUTHORS:

Eleonora Zakharian
University of Illinois at Chicago
57 PUBLICATIONS **538** CITATIONS
SEE PROFILE

Rosetta N. Reusch
Michigan State University
77 PUBLICATIONS **2,063** CITATIONS
SEE PROFILE

Kinetics of Folding of *Escherichia coli* OmpA from Narrow to Large Pore Conformation in a Planar Bilayer†

E. Zakharian and R. N. Reusch*

Department of Microbiology and Molecular Genetics, Michigan State University, East Lansing, Michigan 48824

Received December 28, 2004; Revised Manuscript Received March 2, 2005

ABSTRACT: The outer membrane protein of *Escherichia coli*, OmpA, is currently alleged to adopt two native conformations: a major two-domain conformer in which 171 N-terminal residues form a narrow eight β-barrel pore and 154 C-terminal residues are in the periplasm and a minor one-domain conformer in which all 325 residues create a large pore. However, recent studies in planar bilayers indicate the conformation of OmpA is temperature-sensitive and that increasing temperature converts narrow pores to large pores. Here we examine the reversibility and kinetics of this transition for single OmpA molecules in planar bilayers of diphytanoylphosphatidylcholine (DPhPC). We find that the transition is irreversible. When temperatures are decreased, large pores close down, and when temperatures are stabilized they reopen in the large pore conformation, with gradually increasing open time. Large pores are converted to narrow pores only by denaturing agents. The transition from narrow to large pores requires temperatures $\geq$ 26 °C and is a biphasic process with rates that rise steeply with temperature. The first phase, a flickering stepwise transition from a low-conductance to a high-conductance state requires ~7 h at 26 °C but only ~13 min at 42 °C, signifying an activation energy of 139 ± 12 kJ/mol. This is followed by a gradual increase in conductance and open probability, interpreted as optimization of the large pore structure. The results indicate that the two-domain structure is a partially folded intermediate that is kinetically stable at lower temperatures and that mature fully folded OmpA is a large pore.

OmpA, a major outer membrane protein of *Escherichia coli*, stabilizes the cell envelope (*1*), is a receptor for bacteriophages (*2*, *3*), participates in bacterial conjugation (*4*, *5*), mediates virulence (6, *7*), and is an important target in the immune response (*8*, *9*). OmpA is also a paradigm for studies of the mechanism of insertion, folding, and assembly of integral membrane proteins (*10*−*15*). The current topological model (*16*) for the 325-residue protein maintains that it folds into two alternative conformations: a major two-domain conformer in which N-terminal 171 residues form a narrow eight β-barrel pore in the outer membrane and C-terminal 154 residues associate with the peptidoglycan in the periplasm (*17*, *18*) and a minor conformer in which all 325 residues participate in the production of a large β-barrel pore.

The two-domain conformation of OmpA was proposed on the basis of bacteriophage mapping (*2*, *3*), proteolysis (*20*, *21*), Raman spectroscopy (*22*), and mutagenesis studies (*23*, *24*). The structure of the N-terminal narrow β-barrel pore has been further described by X-ray crystallography (*25*, *26*), NMR (*27*, *28*), and molecular simulations (*29*, *30*). Evidence that OmpA also forms a large pore structure is based on studies by Sugawara and Nikaido (*31*, *32*), which showed that 2−3% of OmpA molecules form nonspecific diffusion pores of ~1 nm diameter in liposomes and planar bilayers studies by Arora et al. (*19*) in which two interconvertible conductance states were observed: a major population of small pores (50−80 pS) and a minor population of large pores (260−320 pS). The large pore conformer was not displayed when only the N-terminal domain was present, indicating that both domains were involved in its formation. It has further been proposed that the large pores oligomerize (*16*). The involvement of the C-terminal domain in pore formation is further supported by studies of OmpA homologues (*33*, *34*) in which antibodies to C-terminal residues revealed exposure of C-terminal epitopes on the cell surface.

Despite this significant evidence for a two-conformer paradigm with narrow pores as majority conformers, we find it incompatible with our recent study (*35*), which indicated that only large high-conductance pores are formed by OmpA in planar bilayers at physiological temperatures. Low-conductance narrow pores were dominant below room temperatures (≤21 °C); however, as temperatures increased, large high-conductance pores made up a greater and greater proportion of the population, and above 37 °C only high-conductance pores were observed. At intermediate temperatures, the two conformers appeared to be interconvertible in the bilayer; however, the reverse transition, i.e., conversion of large pore to narrow pore with decreasing temperature, was not observed.

Here we examine the reversibility of the narrow to large pore transition and the kinetics of the transition as a function of temperature to determine whether the two-domain narrow-pore conformer is indeed a majority native structure or a stable intermediate in a slow folding process.

† Supported by Grant GM 054090 from the National Institutes of Health.

* Corresponding author. Telephone: 517-355-6463. Fax: 517-353-8957. E-mail: rnreusch@msu.edu.

10.1021/bi047278e CCC: $30.25
Published on Web 04/26/2005

MATERIALS AND METHODS

Purification of OmpA Protein. Wild-type OmpA was extracted from outer membranes of *E. coli* JM109 as previously described (*35*). Briefly, stationary-phase cells were suspended in 20 mM Tris-HCl, pH 7.5, 5 mM EDTA and disintegrated by ultrasonication (Branson). The OmpA was extracted from the outer membrane fraction with 2% LiDS, 20 mM Tris-HCl, pH 7.5 and then was loaded onto a column of Sephacryl S-200 (16 × 60, HiPrep, Pharmacia) that had been equilibrated with 0.1% LiDS, 0.4 M LiCl, 20 mM Tris-HCl, pH 7.5. Fractions were eluted with the same solvent and examined by SDS−PAGE. The OmpA was reconstituted into liposomes of C_8E_4 (Sigma Chemical) at a concentration of ca. 80 μg/mL.

SDS−Polyacrylamide Gel Electrophoresis Analysis. OmpA in 20 mM C_8E_4 micelles was incubated alternatively at 22 °C overnight, 37 °C for 1.5 h, 42 °C for 1 h, and 100 °C for 10 min. The protein samples were diluted (1:1, v/v) with loading buffer (0.125 M Tris-Cl, 4% SDS, 20% glycerol, 10% dithiothreitol, 0.2% bromphenol blue) and run on a 12% SDS−PAGE gel. OmpA bands were visualized by staining with Coomassie Brilliant Blue R-250.

Planar Lipid Bilayer Measurements. Planar lipid bilayers were formed from a solution of synthetic diphytanoylphosphatidylcholine (DPhPC,[1] Avanti Polar Lipids, Birmingham, AL) in *n*-decane (Aldrich) (17 mg/mL). The solution was used to paint a bilayer in an aperture of ∼150 μm diameter between aqueous bathing solutions of 1 M KCl in 10 mM Tris, pH 7.1 in a Delrin cup (Warner Instruments, Hamden, CT). All salts were ultrapure (>99%) (Aldrich).

Temperature Studies. For temperature studies, a Teflon cuvette was seated in a special outer chamber made of a polymer/graphite mixture. The chamber was fitted on a conductive stage containing a pyroelectric heater/cooler. Deionized water was circulated through this stage, fed by gravity to remove the heat generated. The pyroelectric heating/cooling stage was driven by a temperature controller (HCC-100A, Dagan Instruments). The temperature of the bath was monitored constantly with a thermoelectric device in the trans side, i.e., the ground side of the cuvette. Although there was a gradient of temperatures between the bath solution and the conductive stage, the temperature within the bath could be reliably controlled to within ±0.5 °C. After the bilayer membrane was formed, 1 μL of 80 μg/mL of OmpA in C_8E_4 micelles was added to the cis compartment, and current fluctuations were observed.

Recording and Data Analysis. Unitary currents were recorded with an integrating patch clamp amplifier (Axopatch 200A, Axon Instruments). The trans solution (voltage command side) was connected to the CV 201A head stage input, and the cis solution was held at virtual ground via a pair of matched AG−AgCl electrodes. Currents through the voltage-clamped bilayers (background conductance < 6 pS) were low-pass-filtered at 10 kHz (−3 dB cutoff, Besel type response) and recorded after digitization through an analog-to-digital converter (Digidata 1322A, Axon Instruments).

[1] Abbreviations: DPhPC, diphytanoylphosphatidylcholine; DOPC, dioleoylphosphatidylcholine; C_8E_4, tetraethylene glycol monooctyl ether; TRDDFQ, time-resolved distance determination by fluorescence quenching; SUV, small unilamellar vesicles; Po, open probability.

Data were filtered through an 8 pole Bessel filter (902LPF, Frequency Devices) and digitized at 1 kHz using pClamp9 software (Axon Instruments). Single-channel conductance events were identified automatically and analyzed by using Clampfit9 software (Axon Instruments). The data were averaged from 10 independent recordings.

RESULTS

Evidence that the Transition from Narrow to Large Pore Conformation Is Irreversible. In a previous study (*35*), we observed the transition of OmpA in planar bilayers from narrow, low-conductance pores (30−139 pS between 15 and 37 °C) to large, high-conductance pores (115−375 pS between 21 and 39 °C). Here we examine further the putative interconvertibility of the narrow and large pore conformers.

We first observed the effects of increasing and decreasing temperatures on single OmpA molecules in the planar bilayer. OmpA, reconstituted in C_8E_4 micelles at room temperature, was incorporated in DPhPC bilayers between aqueous solutions of 1 M KCl in 10 mM Tris, pH 7.1 at 23 °C. Temperature was increased slowly to 37 °C and after a period of 30 min slowly cooled back down to 23 °C. Representative traces taken from 10 independent experiments for each trace are shown in Figure 1. Low-conductance pores (60 ± 20 pS) were predominant at 23 °C (Figure 1A); open probability (Po) was 0.8 (n = 219). As the temperature increased to 37 °C, OmpA was completely converted into large pores in which conductances of 450 ± 70 pS fluctuate with conductances of 500 ± 70 pS. Open probability at 37 °C was high (Po = 0.9; n = 60). When temperatures were decreased, the pores first responded by closure to a very small subconductance state of 6 ± 2 pS (Figure 1Ba). After the temperature was stabilized at 23 °C (∼ 1 h), brief sporadic openings were observed to a large conductance state of 370 ± 50 pS (Po = 0.2; n = 657) (Figure 1Bb). These openings increased in conductance and frequency until after ∼6 h, the conductance was 400 ± 60 pS and Po equal to that at 37 °C (0.9 (n = 1078) Figure 1Bc,d). The low-conductance state was not observed.

Next we examined the effects of temperature on the conformation of OmpA in C_8E_4 micelles. In this study, OmpA was reconstituted into the micelles at the selected temperature. Then, after a period of incubation, the conformation of the protein was determined by observing the single-channel activity of samples incorporated into planar bilayers of the same composition as above at 22 °C. Seven trials were conducted for OmpA incubated at 22 °C for periods of 18−24 h and five for OmpA incubated at 42 °C for periods of 1−2 h. Representative single-channel current records are shown in Figure 2. OmpA incubated at 22 °C has remained in the low-conductance conformation (60 ± 20 pS), whereas OmpA incubated at 42 °C forms only large high-conductance pores (400 ± 60 pS) in the bilayer at 22 °C.

Stability of the Large Pore Conformation of OmpA. The stability of the large pore conformer was further examined by determining the effects of prolonged storage at low temperatures. OmpA-containing micelles were first incubated at 42 °C for 1.5 h to convert all the protein to the large pore conformation. The preparation was then stored at room

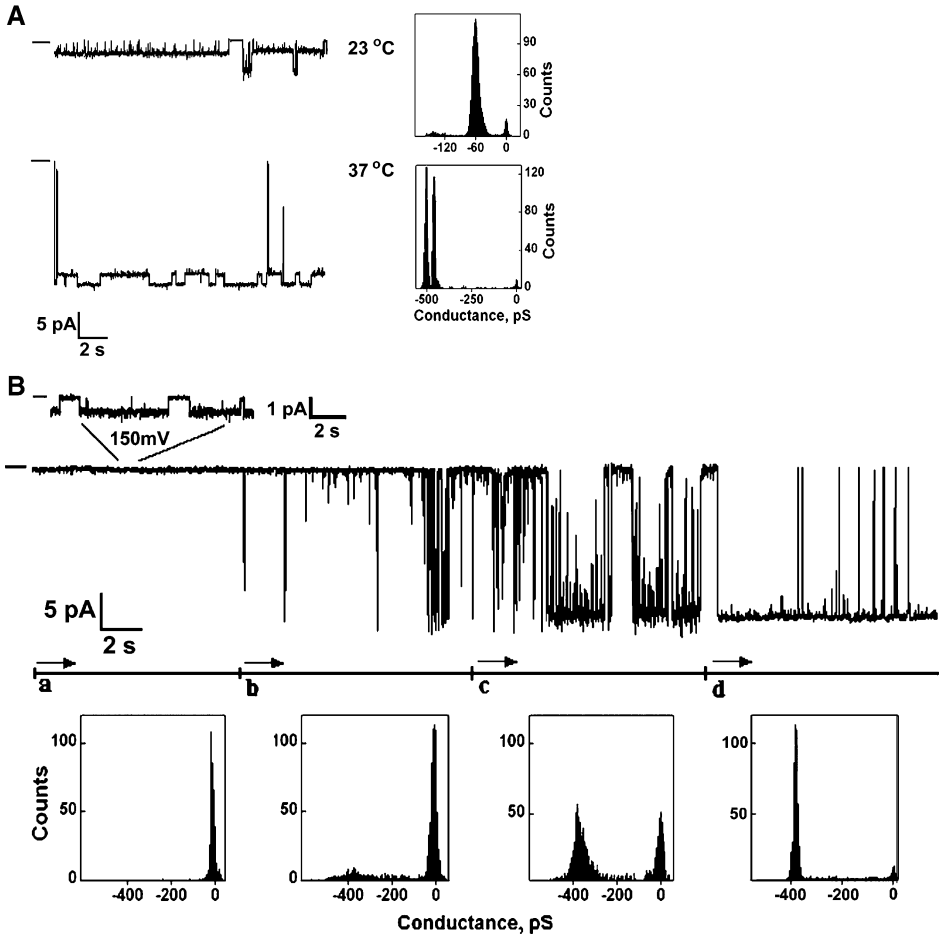

FIGURE 1: Representative single-channel current records showing the effects of temperature on OmpA pores in planar bilayers. The temperature of the chambers was controlled by pyroelectric controller (see Experimental Procedures). The temperature in the cis bath (ground) was read directly using a thermoelectric junction thermometer that also served as a point of reference for the pyroelectric controller. Data were filtered at 1 kHz. Clamping potential was −50 mV. The closed state is delineated by a horizontal bar at the left side of each trace. (A) Effects of increasing temperature. Upper trace: low-conductance currents (60 ± 20 pS) formed by OmpA incorporated into bilayers of DPhPC between symmetric aqueous solutions of 1 M KCl in 10 mM Tris-Cl buffer, pH 7.1 at 23 °C. Lower trace: increasing temperature to 37 °C results in transition to high-conductance currents (450 ± 70 pS). Histograms on right of each trace were taken from longer records (∼10 min each) at the same temperatures. (B) Effect of decreasing temperature. Traces show (a) the closure of the large pore to a very low subconductance state of 6 ± 2 pS when the temperature is decreased from 37 °C; (b−d) stages in the opening of the large pore at 23 °C. (b) ∼1 h; (c) ∼4 h, and (d) ∼6 h). Histograms below each trace were taken from longer records (∼10 min each) obtained under the same conditions.

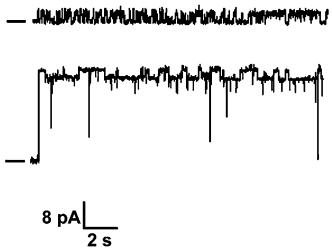

FIGURE 2: Representative single-channel current records showing the effects of preincubation temperature on OmpA pore characteristics. Experimental solutions and procedures are the same as described in the legend to Figure 1. Upper trace: OmpA preincubated at 22 °C for 1 h. Lower trace: OmpA preincubated at 42 °C for 18 h. Clamping potential was +60 mV. The closed state is delineated by a horizontal bar at the left side of each trace.

temperature, 4 °C, or alternatively −20 °C for 18−24 h. The channel activity of each sample was then observed in planar bilayers as above at 22 °C. Four experiments were conducted at each storage temperature. In all cases, OmpA was found entirely in the large pore conformation (400 ± 60 pS) (Figure 3). Observations were repeated after even longer incubation

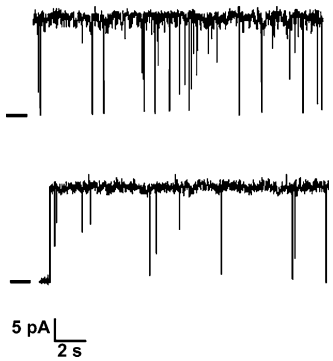

FIGURE 3: Representative single-channel current records showing the effect of storage temperature on OmpA large pores. OmpA in C_8E_4 micelles was preheated at 42 °C for 1.5 h to convert the protein to the large pore structure. Then the micellar solution was incubated either at −20 °C (upper trace) or alternatively at 4 °C (lower trace) for 24 h before incorporation into planar bilayers as in Figure 1 above at 22 °C. Clamping potential was +50 mV. The closed state is delineated by a horizontal bar at the left side of each trace.

times (up to 2 days) with no discernible difference in the pore behavior.

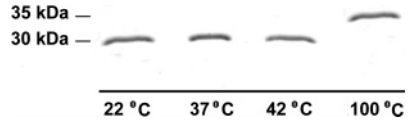

FIGURE 4: Electrophoretic mobility of OmpA conformers on SDS−PAGE gels. OmpA in 20 mM C8E4 micellar solution was incubated overnight at 22 °C, 1.5 h at 37 °C, or 1.5 h at 42 °C. Incubations were stopped by addition of SDS. Samples were not heated before loading. Control sample (100 °C) was boiled in 2% SDS for 10 min. A total of ~7 μg of protein was loaded on each lane.

The effects of denaturing agents on large pore stability was also examined. After incubation at 42 °C as above, the OmpA-containing micelles were incubated in 8 M urea (five trials) or alternatively in 2% SDS (three trials) for 2 days at 22 °C, and the channel activity of each sample was observed in planar bilayers as above. Urea-treated OmpA displayed erratic and irregular current fluctuations indicating complete denaturation, as previously reported by Arora et al. (*19*). However, the large pores exposed to SDS at 22 °C were converted into narrow pores; the current fluctuations were indistinguishable from those in Figure 1A (upper trace).

Electrophoretic Mobility of OmpA Conformers on SDS Gels. Previous studies have shown that the electrophoretic mobility of OmpA on SDS gels depends on the temperature at which the protein is solubilized (*15*). This behavior, referred to as "heat-modifiability" is thought to reflect the protein's conformational state. Accordingly, OmpA is considered denatured when it forms a band at 35 kDa and "native" when it forms a band at 30 kDa.

Here we compared the electrophoretic mobilities of the narrow and large pore conformers of OmpA. Accordingly, OmpA in 20 mM C_8E_4 micellar solution was incubated overnight at 22 °C and alternatively for 1.5 h at 37 and 42 °C. As above, the former sample displayed only low-conductance pores and the latter two samples displayed only high-conductance pores in planar bilayers of DPhPC between aqueous solutions of 1 M KCl in 10 mM Tris, pH 7.1.

The samples were run on SDS−PAGE gels without heating (Figure 4). OmpA, boiled in 2% SDS for 10 min, was used as a control for denatured protein. As shown, both narrow and large pore conformers of OmpA had an apparent MW of 30 kDa, whereas denatured OmpA had an apparent MW of 35 kDa. This indicates that the low- and high-conductance conformers cannot be distinguished by their electrophoretic mobilities; both migrate as "native" protein.

Kinetics of the Narrow to Large Pore Transition in Planar Bilayers as a Function of Temperature. The above experiments indicate that reconstituted OmpA, which has not been exposed to elevated temperature (>25 °C), is in the narrow pore conformation. We may infer that after incorporation into planar bilayers, the protein will open in the narrow pore conformation and rearrange into the large pore conformation only if sufficient heat is applied. These inferences provide the basis for kinetic studies of the transition of single OmpA molecules from narrow to large pore conformation in the planar bilayer as a function of temperature.

Accordingly, the rate of the transition was measured at selected temperatures from 26 to 42 °C. At ≤25 °C, the transition was too slow to measure or did not occur. OmpA-containing micelles were incorporated into planar bilayers as above between aqueous solutions at the temperature of interest. Measurements began with the appearance of irregular current fluctuations, assumed to signal the opening of the narrow pore. Conductance was then followed as a function of time until no further change. As shown in Figure 5A, the rate is steeply temperature-dependent and roughly biphasic. There is an exponential increase in conductance followed by a slow leveling off of conductance. Rate constants (k_{tr}), derived from the initial slopes of the curves, exhibit a linear Arrhenius relationship (Figure 5B), from which an energy of activation of 139 ± 12 kJ/mol was calculated.

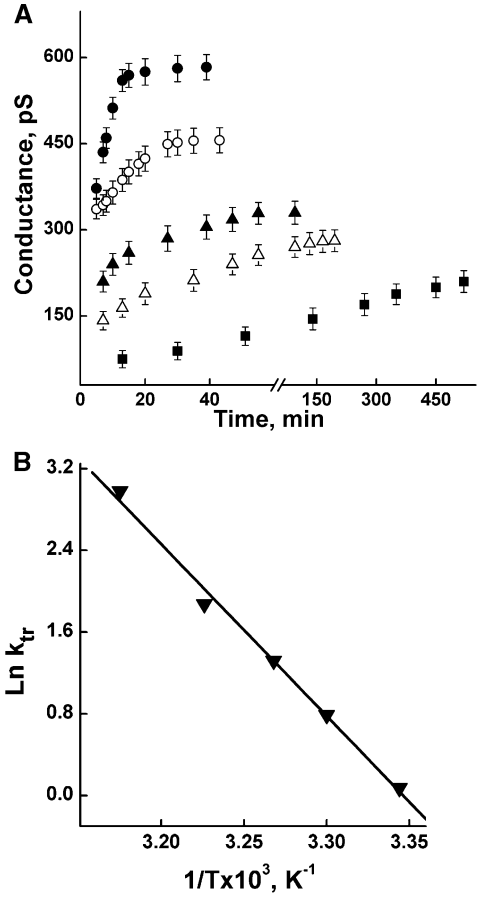

FIGURE 5: (A) Kinetics of the transition of OmpA single channels from narrow to large pore structure at selected temperatures: (■) 26 °C, (△) 30 °C, (▲) 33 °C, (○) 37 °C, and (●) 42 °C. Experimental solutions and procedures are the same as those described in the legend to Figure 1. The data were averaged from at least three experiments at each temperature. (B) Arrhenius plot of rate constants (k_{tr}) obtained from the initial quasi-linear phase of the rate curves in panel A.

Segments of current records, taken from five independent experiments, which illustrate stages in the transition from narrow to large pores at 37 °C, are shown in Figure 6. The process can be divided into two phases, which are conspicuous by the switch in gating mode. In the first phase, the currents rapidly flicker as the pore undergoes small stepwise increases in conductance. This mode extends to about 20 min and corresponds to the linear part of the curve in Figure 5A. In the ~20th minute, the pore closes briefly and then reopens in a different high-conductance gating mode. Conductance and open time continue to increase gradually for another 10 to 20 min. At 37 °C, the conductance at the end of the first phase is ~350 pS, and this increases to ~450 pS at the end of the second phase.

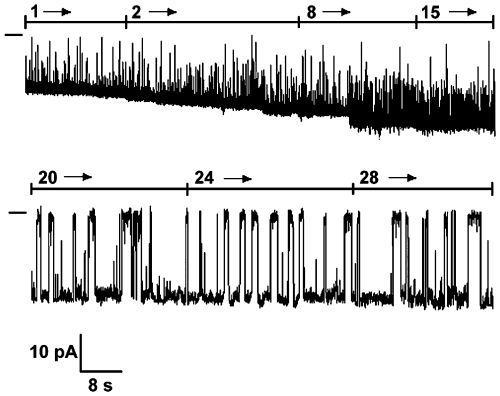

FIGURE 6: Representative single-channel current records of OmpA at constant temperature of 37 °C. The traces are taken from different segments of the transition with initial time in minutes indicated above each trace. Experimental solutions and procedures are the same as those described in the legend to Figure 1. Clamping potential was −60 mV.

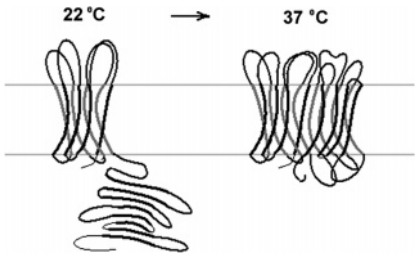

FIGURE 7: Schematic drawing of the transition from a narrow 8 β-barrel pore at lower temperatures to a large hypothetical 16 β-barrel pore at higher temperatures.

DISCUSSION

Our studies establish that the native structure of OmpA in *E. coli* is that of a single-domain large membrane pore (Figure 7). The two-domain structure, which was previously considered to be the majority conformer, is a folding intermediate that is unusually stable at lower temperatures.

In our previous report (*35*), we noted the transition of OmpA from narrow to large pores in planar bilayers as the temperature of the aqueous solutions was increased. Here we find that this process is irreversible. When the conformational rearrangement is completed, the large pore structure is very stable (Figures 1−3). The large pore frequently shows fluctuations between two large conductance states, which may reflect rapid movements of an extracellular loop (Figures 1A and 2). The immediate response of the pore to a decrease in temperature from 37 to 23 °C is closure, presumably due to a block by the extracellular loops (Figure 1B). This block is not complete since a very small subconductance state of 6 ± 2 pS is still evident at higher voltages. When temperature is stabilized, openings to a large conductance state (370 ± 50 pS) reappear sporadically; conductance and open probability then continue to increase gradually for ~6 h and reach values of 400 ± 60 pS and 0.9, respectively. The narrow pore is never observed. Even extended periods at low temperatures do not reverse the transition (Figure 3). Large pores are converted to narrow pores only when they are subjected to denaturing conditions. Apparently, the C-terminal domain is more easily disordered than the N-terminal domain. Treatment with urea or boiling in SDS denatures the entire protein, whereas only the C-terminal domain is denatured by SDS or LiDS at room temperature. The sum of our data indicates strongly that the mature large pore structure is the irreversible end-product of the folding cascade.

Computer modeling studies have supported involvement of the C-terminal domain of OmpA in pore formation. Jeanteur et al. (*36*) predicted two transmembrane β-strands within the C-terminal domain. Additional C-terminal transmembrane segments were predicted by algorithms of Schirmer and Cowan (*37*), and Ferenci (*38*). Stathapoulos (*39*) constructed a 16 β-barrel structure with eight transmembrane segments in the C-terminal domain that is consistent with the varied biochemical, immunological, and genetic topological data concerning OmpA. A large pore structure is also supported by studies of the three-dimensional structure of other outer membrane porins by X-ray crystallography, which indicate they typically form β-barrels with 16 strongly tilted strands (*40*−*43*). We did not observe a tendency for the large conductance pores to oligomerize as has been suggested by Nikaido (*16*), but oligomer formation cannot be ruled out for OmpA in outer membranes that have different lipid components including lipopolysaccharides.

Perhaps the most persuasive evidence for the involvement of the C-terminal domain in pore formation may be found in studies that employed monoclonal antibodies to demonstrate surface exposure of C-terminal residues of OprF in intact cells of *Pseudomonas aeruginosa* (*33*) and OmpA of *Salmonella enterica* (94% identical to *E. coli* OmpA) (*34*). The latter authors found a 2−3-fold increase in binding when the cells were permeabilized to allow access of the antibodies to the periplasm and concluded from this result that only a minor fraction of C-terminal epitopes were exposed on the cell surface. This interpretation supported the view of the two-domain narrow pore as the major conformer. However, there may be other explanations of the data, e.g., the treatment may have increased access to C-terminal epitopes at the extracellular side.

We have also determined the rate of the final folding step as a function of temperature in the range 26 to 42 °C. This folding step was not observed at temperatures < 26 °C. The strong temperature dependence of the transition is indicative of a major conformational rearrangement; the transition requires ~7 h at 26 °C but only ~13 min at 42 °C. The activation energy, estimated as 139 ± 12 kJ/mol for the folding of the narrow to the large pore in DPhPC planar bilayers (Figure 5B), is considerably higher than the 46.4 ± 3.8 kJ/mol reported by Kleinschmidt and Tamm (*11*) for the folding of denatured OmpA to the native form in DOPC SUV micelles as determined by tryptophan fluorescence. This difference may partly reflect the greater curvature and fluidity of the DOPC micelles (*15*) and perhaps also the lower energy barrier for a folding process in which the eight β-barrel narrow pore is a transient and thereby less ordered structure. Our experience and that of others (*19*) indicates that pores formed by urea-denatured OmpA are much less structured than pores formed by OmpA subjected to SDS or LDS at or below room temperature. In the cell, the folding process may be assisted by chaperones that lower the activation energy still further.

Most previous studies of OmpA structure were conducted at room temperature or below. In this temperature range, folding is incomplete and the two-domain conformer is the sole or predominant product of the folding process; thus it

is not surprising that the large pore conformer was not observed. However, Kleinschmidt and Tamm (*12*−*14*) followed the kinetics of membrane insertion and folding of urea-denatured OmpA in dioleoylphosphatidylcholine (DOPC) bilayers as a function of temperature by changes in electrophoretic mobility and tryptophan fluorescence. We find many points of agreement with their results, albeit with some differences in interpretation of the data.

In gel shift studies, Kleinschmidt and Tamm (*12*−*14*) followed the rate at which the electrophoretic mobility of OmpA on SDS gels changed from 35 kDa, characteristic of the denatured form, to 30 kDa, attributed to the "native" form, which was considered to be the two-domain narrow pore. The rates were strongly temperature-dependent; the process required 8 h at 20 °C, 1 h at 30 °C, and 30 min at 40 °C. In light of our results here, which show no detectable difference in electrophoretic mobility between narrow and large pore conformers (Figure 4), we suggest their data agree with an interpretation in which the narrow pore conformer was the final product at 20 °C but that folding undiscernibly progressed to the large pore conformer at the higher temperatures.

Kleinschmidt and Tamm also observed folding of urea-denatured OmpA into DOPC micelles (SUVs) using time-resolved distance determination by fluorescence quenching (TRDDFQ). They observed three kinetic steps: a fast temperature-independent step and two slow temperature-dependent steps, which designated three membrane-bound intermediates leading to the native state. In the first intermediate, the five tryptophans, all of which are located in the narrow pore domain, remained 14−15 Å from the center of the bilayer. Consequently, the first step was attributed to binding of denatured OmpA to the bilayer surface. In the second intermediate, the tryptophans were ∼10 Å from the bilayer center. In the third intermediate, the tryptophans had become delocalized, their average position being in the center of the bilayer. In the final native state, the tryptophans are again ∼10 Å from the bilayer center. Interestingly, the third intermediate and subsequent native state were kinetically accessible only at temperatures ≥ 26 °C.

Our kinetic measurements began at each set temperature with the first display of low-conductance current fluctuations; thus OmpA was initially in the narrow pore conformation, and earlier stages, such as membrane absorption or preliminary insertion steps, were unobserved in our study. Our measurements ended when there were no further significant changes in conductivity or gating. Accordingly, we may reasonably infer that we were observing the folding of single OmpA molecules from the narrow to large pore conformations (Figure 7). Since our studies begin with OmpA already in the narrow pore conformation and the fluorescence studies of Kleinschmidt and Tamm with denatured OmpA, we propose that our initial current fluctuations correspond roughly to their second intermediate, in which the five tryptophans are ∼10 Å from the bilayer center. Kleinschmidt and Tamm assume them to be on the cis side of the bilayer; however, their method does not distinguish cis and trans locations. Our analysis implies that four of the tryptophans have crossed the center of the bilayer and reached the trans side, placing them and the fifth tryptophan (cis side) in the approximate position of the tryptophans (9−10 Å) in the crystal and NMR structures of the eight β-barrel narrow pore (*23*−*26*).

In both the planar bilayer and fluorescence studies, the second intermediate is stabilized at temperatures up to 25 °C; there is no significant change in conductance or further movement of tryptophans, which supports our view that the structure is in the stable narrow-pore conformation. At temperatures ≥ 26 °C, OmpA exhibits flickering currents in the bilayer that increase stepwise in amplitude with time (Figure 6, 1−19 min), interpreted as intermittent trial insertions intermingled with successful insertions of segments of the C-terminal domain, resulting in the gradual enlargement of the pore diameter and ending with an abrupt closure. This phase correlates to the delocalization of tryptophans during formation of the third intermediate. Both events may signal disruption of the eight β-barrel pore by insertion of C-terminal segments into the bilayer and restructuring of the protein into a large pore. The pore reopens in the second phase as a large pore in a different gating mode. The subsequent slow increases in conductance (Figure 6, 20−28 min) and matching movement of tryptophans to a position ∼10 Å from the center of the bilayer, presumably trans, may then reflect the optimization of the native large pore structure. This phase closely resembles the reopening of the large pore after a drop in temperature to 23 °C (Figure 1B) but at a much quicker pace as expected at the higher temperature.

In summary, we have observed the final stage of OmpA folding from a two-domain narrow pore to a single-domain large pore in a planar bilayer as a function of time and temperature. We find that this folding step is irreversible and steeply temperature-dependent, requiring temperatures ≥ 26 °C in vitro due to its high activation energy (∼139 kJ/mol). A large pore structure for OmpA is consistent with structures of other outer membrane porins (*40*−*43*) and with known functions of OmpA as a receptor for bacteriophages (*1*−*3*), which suggest it may serve as a conduit for large organic molecules such as ssDNA.

REFERENCES

1. Sonntag, I., Schwarz, H., Hirota, Y., and Henning, U. (1978) Cell envelope and shape of *Escherichia coli*: multiple mutants missing the outer membrane lipoprotein and other major outer membrane proteins, *J. Bacteriol. 136*, 280−285.
2. Morona, R., Klose, M., and Henning, U. (1984) *Escherichia coli* K-12 outer membrane protein (OmpA) as a bacteriophage receptor: analysis of mutant genes expressing altered proteins, *J. Bacteriol. 159*, 570−578.
3. Morona, R., Krämer, C., and Henning, U. (1985) Bacteriophage receptor area of outer membrane protein OmpA of *Escherichia coli* K-12, *J. Bacteriol. 164*, 539−564.
4. Schweizer, M., and Henning, U. (1977) Action of a major cell envelope membrane protein in conjugation of *Escherichia coli* K12, *J. Bacteriol. 129*, 1651−1652.
5. Ried, G., and Henning, U. (1987) A unique amino acid substitution in the outer membrane protein OmpA causes conjugation deficiency in *Escherichia coli* K-12, *FEBS Lett. 223*, 387−390.
6. Khan, N. A., Shin, S., Chung, J. W., Kim, K. J., Elliott, S., Wang, Y., Kim, K. S. (2003) Outer membrane protein A and cytotoxic necrotizing factor-1 use diverse signaling mechanisms for *Escherichia coli* K1 invasion of human brain microvascular endothelial cells, *Microb. Pathog. 35*, 35−42.
7. Xie, Y., Kim, K. J., and Kim, K. S. (2004) Current concepts on *Escherichia coli* K1 translocation of the blood-brain barrier, *FEMS Immunol. Med. Microbiol. 42*, 271−279.
8. Godefroy, S., Corvaia, N., Schmitt, D., Aubry, J. P., Bonnefoy, J. Y., Jeannin, P., and Staquet, M. J. (2003) Outer membrane protein

A (OmpA) activates human epidermal Langerhans cells, *Eur. J. Cell. Biol. 82*, 193−200.
9. Jeannin, P., Magistrelli, G., Herbault, N., Goetsch, L., Godefroy, S., Charbonnier, P., Gonzalez, A., and Delneste, Y. (2003) Outer membrane protein A renders dendritic cells and macrophages responsive to CCL21 and triggers dendritic cell migration to secondary lymphoid organs, *Eur. J. Immun. 32*, 326−332.
10. Klose, M., Schwarz, H., MacIntyre, S., Freudl, R., Eschbach, M., and Henning, U. (1988) Internal deletions in the gene for an *Escherichia coli* outer membrane protein define an area possibly important for recognition of the outer membrane by this polypeptide, *J. Biol. Chem. 263*, 13291−13296.
11. Kleinschmidt, J. H., and Tamm, L. K. (1996) Folding intermediates of a beta-barrel membrane protein. Kinetic evidence for a multistep membrane insertion mechanism, *Biochemistry 35*, 12993−13000.
12. Kleinschmidt, J. H., and Tamm, L. K. (1999) Time-resolved distance determination by tryptophan fluorescence quenching: probing intermediates in membrane protein folding, *Biochemistry 38*, 4996−5005.
13. Kleinschmidt, J. H., den Blaauwen, T., Driessen, A. J., and Tamm, L. K. (1999) Outer membrane protein A of *Escherichia coli* inserts and folds into lipid bilayers by a concerted mechanism, *Biochemistry 38*, 5006−5016.
14. Tamm, L. K., Arora, A., and Kleinschmidt, J. H. (2001) Structure and assembly of β-barrel membrane proteins, *J. Biol. Chem. 276*, 32399−32402.
15. Surrey, T., and Jähnig, F. (1995) Kinetics of folding and membrane-insertion of a β-barrel membrane protein, *J. Biol. Chem. 270*, 28199−28203.
16. Nikaido, H. (2003) Molecular basis of bacterial outer membrane permeability revisited, *Microbiol. Mol. Biol. Rev. 67*, 593−656.
17. DeMot, R., and Vanderleyden, J. (1994) The C-terminal sequence conservation between OmpA-related outer membrane proteins and MotB suggests a common function in both gram-positive and gram-negative bacteria, possibly in the interaction of these domains with peptidoglycan, *Mol. Microbiol. 12*, 333−354.
18. Koebnik, R. (1995) Proposal for a peptidoglycan-associating alpha-helical motif in the C-terminal regions of some bacterial cell-surface proteins, *Mol. Microbiol. 16*, 1269−1270.
19. Arora, A., Rinehart, D., Szabo, G., and Tamm, L. K. (2000) Refolded outer membrane protein A of *Escherichia coli* forms ion channels with two conductance states in planar lipid bilayers, *J. Biol. Chem. 275*, 1594−1600.
20. Schweizer, M., Hindennach, I., Garten, W., and Henning, U. (1978) Major proteins of the *Escherichia coli* outer cell envelope membrane. Interaction of protein II with lipopolysaccharide, *Eur. J. Biochem. 82*, 211−217.
21. Ried, G., Koebnik, R., Hindennach, I., Mutschler, B., and Henning, U. (1994) Membrane topology and assembly of the outer membrane protein OmpA of *Escherichia coli* K12, *Mol. Gen. Genet. 243*, 127−135.
22. Vogel, H., and Jähnig, F. (1986) Models for the structure of outer-membrane proteins of *Escherichia coli* derived from Raman spectroscopy and prediction methods, *J. Mol. Biol. 190*, 191−199.
23. Koebnik, R. (1999) Membrane assembly of the *E. coli* outer membrane protein OmpA: exploring sequence constraints on transmembrane β-strands, *J. Mol. Biol. 285*, 1801−1810.
24. Koebnik, R. (1999) Structural and functional roles of the surface-exposed loops of the β-barrel membrane protein OmpA from *Escherichia coli*, *J. Bacteriol. 181*, 3688−3694.
25. Pautsch, A., and Schulz, G. E. (1998) Structure of the outer membrane protein A transmembrane domain, *Nat. Struct. Biol. 5*, 1013−1017.
26. Pautsch, A., and Schulz, G. E. (2000) High-resolution structure of the OmpA membrane domain, *J. Mol. Biol. 298*, 273−282.
27. Arora, A., Abildgaard, F., Bushweiler, J. H., and Tamm, L. K. (2001) Structure of outer membrane protein A transmembrane domain by NMR spectroscopy, *Nat. Struct. Biol. 8*, 334−336.
28. Fernandez, C., Hilty, C., Bonjour, S., Adeishvili, K., Pervushin, K., and Wüthrich, K. (2001) Solution NMR studies of the integral membrane proteins OmpX and OmpA from *Escherichia coli*, *FEBS Lett. 504*, 173−178.
29. Bond, P. J., Faraldo-Gomez, J. D., and Sansom, M. S. (2002) OmpA: a pore or not a pore? Simulation and modeling studies, *Biophys. J. 83*, 763−75.
30. Domene, C., Bond, P. J., and Sansom, M. S. (2003) Membrane protein simulations: ion channels and bacterial outer membrane proteins, *Adv. Protein Chem. 66*, 159−93.
31. Sugawara, E., and Nikaido, H. (1992) Pore-forming activity of OmpA protein of *Escherichia coli*, *J. Biol. Chem. 267*, 2507−2511.
32. Sugawara, E., and Nikaido, H. (1994) OmpA protein of *Escherichia coli* outer membrane occurs in open and closed channel forms, *J. Biol. Chem. 269*, 17981−17987.
33. Rawling, E. G., Martin, N. L., and Hancock, R. E. W. (1995) Epitope mapping of the *Pseudomonas aeruginosa* major outer membrane porin protein OprF, *Infect. Immun. 63*, 38−42.
34. Singh, S. P., Williams, Y. U., Miller, S., and Nikaido, H. (2003) The C-terminal domain of *Salmonella enterica* serovar typhimurium OmpA is an immunodominant antigen in mice but appears to be only partially exposed on the bacterial cell surface, *Infect. Immun. 71*, 3937−3946.
35. Zakharian, E., and Reusch, R. N. (2003) Outer membrane protein A of *Escherichia coli* forms temperature-sensitive channels in planar lipid bilayers, *FEBS Lett. 555*, 229−235.
36. Jeanteur, D., Lakey, J. H., and Pattus, F. (1994) in *Bacterial Cell Wall* (Ghuysen, J. M., and Hakenbeck, R., Eds.) pp 363−379, Elsevier Science, Amsterdam.
37. Schirmer, T., and Cowan, S. W. (1993) Prediction of membrane-spanning beta-strands and its application to maltoporin, *Protein Sci. 2*, 1361−1363.
38. Ferenci, T. (1994) From sequence alignment to structure prediction: the case of the OmpF porin family, *Mol. Microbiol. 14*, 188−189.
39. Stathopoulos, C. (1996) An alternative topological model for *Escherichia coli* OmpA, *Protein Sci. 5*, 170−173.
40. Cowan, S. W., Schirmer, T., Rummel, G., Steriet, M., Ghosh, R., Pauptit, A., Jansonius, J. N., and Rosenbusch, J. P. (1992) Crystal structures explain functional properties of two *Escherichia coli* porins, *Nature 358*, 727−733.
41. Weiss, M. S., and Schulz, G. E. (1992) Structure of porin refined at 1.8 Å resolution, *J. Mol. Biol. 227*, 493−509.
42. Koebnik, R., Locher, K. P., and Van Gelder, P. (2000) Structure and function of bacterial outer membrane proteins: barrels in a nutshell, *Mol. Microbiol. 37*, 239−253.
43. Schulz, G. (2002) The structure of bacterial outer membrane proteins, *Biochim. Biophys. Acta 1565*, 308−317.

BI047278E